

-Project 3 - FYS3150/FYS4150-

By Simon Schrader (4150), Adrian Kleven (3150) - autumn 2019

Contents

List of Figures	2
List of Tables	2
1 Abstract	3
2 Introduction	3
3 Methods	4
3.1 Gaussian quadrature	4
3.1.1 Gauss- Legendre quadrature	6
3.1.2 Gauss- Laguerre quadrature	7
3.2 Monte Carlo Integration	9
3.3 Application	10
3.3.1 Legendre polynomials	10
3.3.2 Laguerre and Legendre polynomials	11
3.3.3 Monte Carlo integration without importance sampling . .	12
3.3.4 Monte Carlo integration with importance sampling	12
3.4 Computational implementation	13
3.4.1 Parallelization	13
4 Results	14
4.1 Legendre polynomials	14
4.2 Laguerre and Legendre polynomials	14
4.3 Cartesian Monte Carlo without importance sampling	15
4.4 Spherical Monte Carlo with importance sampling	16
4.5 Time usage and parallelization	16
5 Conclusion	19
6 Appendix	20
6.1 Proof that \mathbf{L} is invertible	20
6.2 Proof that $F^{-1}(U)$ has cumulative function $F(x)$	20
6.3 Monte Carlo relative error improvement with importance sampling	20
6.4 Monte Carlo time expenditure increase with importance sampling	21
6.5 List of programs	21
7 References	22

List of Figures

1	Plot of function	11
2	Time vs. relative error	17
3	N vs. relative time use	18
4	Vectorization flags	19

List of Tables

1	Cartesian Quadrature using Legendre polynomials	14
2	Spherical Quadrature using Laguerre polynomials	15
3	Cartesian Monte Carlo without importance sampling	15
4	Spherical Monte Carlo with importance sampling	16

1 Abstract

Determining the ground state correlation energy between two electrons in a helium atom can be done by evaluating a certain six- dimensional integral assuming that the electrons can be modelled separately, as two, single- particle wave functions of an electron in the hydrogen atom [3]. This integral is also applicable in other aspects of quantum mechanics [3]. To solve this integral, two different approaches relying on Gaussian quadrature and Monte Carlo integration were used, as well as the implementation of parallelization to speed up the programs.

Gauss- quadrature proved was only accurate within 1%.Both implementations of Monte Carlo integration proved to be a lot more effective than Gaussian quadrature both in accuracy and time expenditure (see figure 2). Monte Carlo integration with importance sampling gave the best results which is $0.192784 \pm 3.287 \cdot 10^{-5}$ with 10^9 mesh points and also proved best in terms of time v. accuracy. The addition of parallel computing sped the process up by over 350% given 10^7 mesh points. See figure 3.

2 Introduction

The purpose of this article is to apply different versions of Gaussian quadrature and Monte Carlo integration in solving the six- dimensional integral

$$\int_{-\infty}^{\infty} \int_{-\infty}^{\infty} \int_{-\infty}^{\infty} \int_{-\infty}^{\infty} \int_{-\infty}^{\infty} \int_{-\infty}^{\infty} f(x_1, x_2, y_1, y_2, z_1, z_2) dx_1 dx_2 dy_1 dy_2 dz_1 dz_2$$

Where

$$f(x_1, x_2, y_1, y_2, z_1, z_2) = \frac{\exp\left(-4\left(\sqrt{x_1^2 + y_1^2 + z_1^2} + \sqrt{x_2^2 + y_2^2 + z_2^2}\right)\right)}{\sqrt{(x_1 - x_2)^2 + (y_1 - y_2)^2 + (z_1 - z_2)^2}} \quad (1)$$

to examine their times expenditure and accuracy, as well as the effect of parallelizing the C++ implementations of these methods. This integral has the known analytical solution $5\pi^2/16^2$.

Gauss- Legendre and Gauss- Laguerre quadrature takes advantage of two different sets of polynomials, orthogonal under some inner product, and applicable on two different types of intervals. By applying either the Gauss- Legendre quadrature or the Gauss- Laguerre quadrature to the integral (possibly after some change of variables or coordinate system), it's possible to benchmark each of their respective accuracies with the analytical result of the integral as well as compare their time expenditure.

We compared the Gauss- quadratures with Monte Carlo integration. In addition, this article will examine the effectiveness of importance sampling in Monte Carlo integration, its impact on time expenditure and how much faster it converges towards the real value.

3 Methods

The expectation value of the correlation energy between two electrons interacting under the Coulomb interacting is given by the integral

$$\left\langle \frac{1}{|\mathbf{r}_1 - \mathbf{r}_2|} \right\rangle = \int_{-\infty}^{\infty} d\mathbf{r}_1 d\mathbf{r}_2 e^{-2\alpha(r_1+r_2)} \frac{1}{|\mathbf{r}_1 - \mathbf{r}_2|}. \quad (2)$$

where

$$\mathbf{r}_i = x_i \mathbf{e}_x + y_i \mathbf{e}_y + z_i \mathbf{e}_z$$

and

$$r_i = \sqrt{x_i^2 + y_i^2 + z_i^2}.$$

$\alpha = 2$, corresponding to the charge of the nucleus of the helium atom as given by [3].

3.1 Gaussian quadrature

The method of Gaussian quadrature allows one to approximate a function $f(x)$ with a polynomial $P_{2N-1}(x)$ of degree $2N-1$, using only N mesh points. Said polynomial is constructed using sets of orthogonal polynomials, meaning they have the property that

$$\int_a^b P_i(x) P_j(x) W(x) dx = C_{ij} \delta_{ij} \quad (3)$$

where $\{P_k \mid k \in \mathbb{N}\}$ is the set of polynomials orthogonal in the domain $[a, b]$, δ_{ij} is the Kronecker- delta and $P_0(x)$ is normalized to be 1. C_{ij} is a normalization constant specific for the polynomial in question. $W(x)$ a function associated with the particular inner product by which the polynomials are orthogonal. This will equal 1 for now, as we deal with that specific inner product relating to the Legendre- polynomials.

Since the polynomials $\{P_k \mid k \in \{0, \dots, N\}\}$ constitute an orthogonal set, any polynomial of degree N or less can be constructed by a linear combination them

Suppose a function $f(x)$ is approximated by the polynomial Q_{2N-1} . Then

$$\int_a^b f(x) dx \approx \int_a^b Q_{2N-1}(x) dx = \int_a^b (P_N(x) Q_{N-1}(x) + R_{N-1}(x)) dx \quad (4)$$

where, due to the orthogonality of the P_k 's, Q_{2N-1} can be decomposed into P_N R_{N-1} and

$$Q_{N-1} = \sum_{k=0}^{N-1} \beta_k P_k. \quad (5)$$

Then

$$\sum_{k=0}^{N-1} \left(\int_a^b \beta_k P_N(x) P_k(x) dx \right) + \int_a^b R_{N-1}(x) dx = \int_a^b R_{N-1}(x) dx$$

so

$$\int_a^b f(x) dx \approx \int_a^b R_{N-1}(x) dx = \sum_{k=0}^{N-1} \int_a^b \alpha_k P_k(x) dx$$

where R_{N-1} has been expressed in terms of orthogonal polynomials as was done in equation 5. Inserting $P_0(x) = 1$ this expression can be rewritten, then simplified:

$$\int_a^b R_{N-1}(x)dx = \sum_{k=0}^{N-1} \int_a^b \alpha_k P_0(x) P_k(x) dx = \int_a^b \alpha_0 = \alpha_0(b-a). \quad (6)$$

So it's only necessary to identify a single coefficient when evaluating this integral. Looking again at the polynomial $Q_{2N-1}(x)$ that serves as the approximation to the function $f(x)$. The points x_n where $n \in \{0, \dots, N-1\}$ are the zeros of P_N . Composing the polynomial as was done in equation 4

$$Q_{2N-1}(x) = P_N(x)Q_{N-1}(x) + R_{N-1}(x)$$

and assessing at the points x_n :

$$Q_{2N-1}(x_n) = P_N(x_n)Q_{N-1}(x_n) + R_{N-1}(x_n) = R_{N-1}(x_n). \quad (7)$$

So at the zeros of P_N , the approximating polynomial $Q_{2N-1}(x)$ equals $R_{N-1}(x)$ which as the other polynomials, can be expressed as a linear combination of orthogonal polynomials as was done in equation 5.

$$R_{N-1}(x) = \sum_{k=0}^{N-1} \alpha_k P_k(x).$$

And at the points x_n :

$$R_{N-1}(x_n) = \sum_{k=0}^{N-1} \alpha_k P_k(x_n) \quad n \in \{0, \dots, N-1\}. \quad (8)$$

As $\{P_k \mid k \in \{0, \dots, N\}\}$ are orthogonal polynomials, no single P_k is linearly dependent on any others, thus $P_k(x_n)$ can be expressed as an invertible $N \times N$ matrix with matrix elements P_{kn} (see Appendix 6.1).

Multiplying both sides of equation 8 by

$$\sum_{j=0}^{N-1} P_{jk}^{-1} \quad (9)$$

yields

$$\left(\sum_{j=0}^{N-1} P_{jk}^{-1} \right) R_{N-1}(x_n) = \left(\sum_{j=0}^{N-1} P_{jk}^{-1} \right) \sum_{k=0}^{N-1} \alpha_k P_k(x_n)$$

which, due to the orthogonality of the column- vectors gives

$$\sum_{k=0}^{N-1} P_{nk}^{-1} R_{N-1}(x_k) = \alpha_n. \quad (10)$$

Returning then to equation 6, and inserting the expression 10 for $n = 0$.

$$\int_a^b R_{N-1}(x)dx = (b-a) \left(\sum_{k=0}^{N-1} P_{0k}^{-1} R_{N-1}(x_k) \right). \quad (11)$$

Remembering back to equation 7 and labelling $\omega_k = (b-a)P_{0k}^{-1}$ as the weights, the final equation is arrived at:

$$\int_a^b f(x)dx \approx \int_a^b Q_{2N-1}(x)dx = \sum_{k=0}^{N-1} \omega_k Q_{2N-1}(x_k) \quad (12)$$

where x_k are the N zeros of the orthogonal polynomial P_N of degree N , Q_{2N-1} is the polynomial approximation of the original function $f(x)$ and ω_k are the associated weights.

For the case of $-a = b = 1$, the orthogonal polynomials in question are the Legendre polynomials, orthogonal in the interval $x \in \{-1, \dots, 1\}$. Other such polynomials, orthogonal on different intervals, such as the Laguerre polynomials can be applied in the same manner, although come attached with an associated weight function $\{W(x) \mid W(x) > 0, x \in \{-1, \dots, 1\}\}$, integrable on the interval $[a, b]$ such that the integral to be evaluated is

$$\int_a^b W(x)f(x)dx$$

[2].

3.1.1 Gauss- Legendre quadrature

Expressing the integral in equation 2 in terms of x_1, y_1, z_1 and x_2, y_2, z_2 :

$$\iiint_{-\infty}^{\infty} \iiint_{-\infty}^{\infty} \frac{\exp\left(-4\left(\sqrt{x_1^2 + y_1^2 + z_1^2} + \sqrt{x_2^2 + y_2^2 + z_2^2}\right)\right)}{\sqrt{(x_1 - x_2)^2 + (y_1 - y_2)^2 + (z_1 - z_2)^2}} dx_1 dx_2 dy_1 dy_2 dz_1 dz_2 \quad (13)$$

The Gauss- Legendre quadrature relies on the orthogonality of the Legendre polynomials in the domain $x \in \{-1, \dots, 1\}$. Therefore it's necessary to replace infinity with other bounds that still yield suitable results. Then, only a simple change of variables is required to bring the integration bounds to $[-1, 1]$:

$$\lim_{t \rightarrow \pm\infty} f(t) \approx f(\pm\lambda)$$

change of variable $t = \lambda\tau$:

$$\int_{-\lambda}^{\lambda} f(t)dt = \lambda \int_{-1}^1 f(\lambda\tau)d\tau$$

Using this fact for integral 13 gives

$$\lambda^5 \iiint_{-1}^1 \iiint_{-1}^1 \frac{\exp\left(-4\lambda\left(\sqrt{\chi_1^2 + v_1^2 + \zeta_1^2} + \sqrt{\chi_2^2 + v_2^2 + \zeta_2^2}\right)\right)}{\sqrt{(\chi_1 - \chi_2)^2 + (v_1 - v_2)^2 + (\zeta_1 - \zeta_2)^2}} d\chi_1 d\chi_2 dv_1 dv_2 d\zeta_1 d\zeta_2$$

and then renaming the integrand

$$g(\chi_1, \chi_2, v_1, v_2, \zeta_1, \zeta_2) = \frac{\exp\left(-4\lambda\left(\sqrt{\chi_1^2 + v_1^2 + \zeta_1^2} + \sqrt{\chi_2^2 + v_2^2 + \zeta_2^2}\right)\right)}{\sqrt{(\chi_1 - \chi_2)^2 + (v_1 - v_2)^2 + (\zeta_1 - \zeta_2)^2}} \quad (14)$$

gives the final equation

$$\lambda^5 \iiint_{-1}^1 \iiint_{-1}^1 \iiint_{-1}^1 g(\chi_1, \chi_2, v_1, v_2, \zeta_1, \zeta_2) d\chi_1 d\chi_2 dv_1 dv_2 d\zeta_1 d\zeta_2. \quad (15)$$

As long as the function g can be approximated with a polynomial P_{2N-1} of degree $2N-1$ or lower on the interval $[-1, 1]$, this integral can be approximated by

$$\lambda^5 \sum_{i_1=1}^N \cdots \sum_{i_6=1}^N \omega_{i_1} \cdots \omega_{i_6} g(x_{i_1}, \cdots, x_{i_6}) \quad (16)$$

where ω_{ik} for $k \in \{1, \cdots, 6\}$ are the weights and x_{ik} for $k \in \{1, \cdots, 6\}$ are the zeros of the Legendre polynomial \mathcal{L}_N of degree N .

$\mathcal{L}_N(x_{ik})$ can be gotten by simply using the recursion relation

$$(n+1)\mathcal{L}_{n+1}(x_{ik}) + n\mathcal{L}_{n-1}(x_{ik}) - (2n+1)x_{ik}\mathcal{L}_n(x_{ik}) = 0 \quad (17)$$

given by [2] and the requirement that $\mathcal{L}_0 = 1$.

The zeros of \mathcal{L}_N , x_{ik} are found by any root-finding algorithm, such as Newton's method.

3.1.2 Gauss- Laguerre quadrature

The Gauss- Legendre quadrature in this case, got a little tricky. A different approach would be to transform the integral with polar coordinates and using the Laguerre polynomials that are orthogonal on the interval $[0, \infty]$.

Looking again at equation 2, and applying the change of variables given in the Project 3 Problem set [3] section 3b):

$$\int_0^\pi \int_0^\pi \int_0^{2\pi} \int_0^{2\pi} \int_0^\infty \int_0^\infty \frac{r_1^2 r_2^2 \sin(\theta_1) \sin(\theta_2) e^{-4(r_1+r_2)}}{\sqrt{r_1^2 + r_2^2 - 2r_1 r_2 \cos(\beta)}} dr_1 dr_2 d\phi_1 d\phi_2 d\theta_1 d\theta_2 \quad (18)$$

with

$$\cos(\beta) = \cos(\theta_1)\cos(\theta_2) + \sin(\theta_1)\sin(\theta_2)\cos(\phi_1 - \phi_2).$$

r_1 and r_2 in this case, are integrated from 0 to ∞ , suitable for the Gauss-Laguerre quadrature.

The Gauss- Laguerre quadrature carries the weight function

$$W(x) = x^\alpha e^{-x} \quad (19)$$

[2]. α being the exponent of x in an integral of the form

$$\int_0^\infty x^\alpha e^{-x} f(x). \quad (20)$$

For simplicity, lets isolate one of the r 's in the integrand, as the other will be treated as a constant. let's pick r_1 :

$$C \int_0^\infty \frac{r_1^2 e^{-4r_1}}{\sqrt{r_1^2 + r_2^2 - 2r_1 r_2 \cos(\beta)}} dr_1 \quad (21)$$

where

$$C = \int_0^\pi \int_0^\pi \int_0^{2\pi} \int_0^{2\pi} \int_0^\infty r_2^2 \sin(\theta_1) \sin(\theta_2) e^{-4r_2} dr_2 d\phi_1 d\phi_2 d\theta_1 d\theta_2.$$

The integral 21, can then be written as

$$C \int_0^\infty W(r_1) R(r_1) dr_1 \quad (22)$$

with

$$W(r_1) = r_1^2 e^{-r_1}$$

and

$$R(r_1) = \frac{e^{-3r_1}}{\sqrt{r_1^2 + r_2^2 - 2r_1 r_2 \cos(\beta)}}.$$

Integral 22, neglecting C for just a bit, can now be approximated according to the Gauss- Laguerre quadrature:

$$\begin{aligned} \int_0^\infty g(x) dx &= \int_0^\infty W(x) f(x) dx \approx \int_0^\infty e^{-x} Q_{2N-1}(x) dx \\ &= \int_0^\infty e^{-x} (P_N(x) Q_{N-1}(x) + R_{N-1}(x)) dx = \int_0^\infty e^{-x} R_{N-1}(x) dx \\ &= \int_0^\infty e^{-x} R_{N-1}(x) dx = \sum_{k=0}^{N-1} \int_0^\infty e^{-x} \alpha_k L_0(x) L_k(x) dx = \int_0^\infty \alpha_0 e^{-x} L_0 L_0 dx \\ &= \int_0^\infty e^{-x} R_{N-1}(x) dx = \int_0^\infty \alpha_0 e^{-x} dx = \alpha_0 \end{aligned} \quad (23)$$

Determining the coefficient α_0

$$e^{-x_n} Q_{2N-1}(x_n) = e^{-x_n} (L_N(x_n) Q_{N-1}(x_n) + R_{N-1}(x_n)) = e^{-x_n} R_{N-1}(x_n).$$

where x_n are the zeros of L_N .

$$e^{-x_n} R_{N-1}(x_n) = \sum_{k=0}^{N-1} \alpha_k e^{-x_n} L_k(x_n) \quad n \in \{1, \dots, N\}. \quad (24)$$

Gives the matrix \mathbf{L} with matrix elements \mathbf{L}_{kn} :

$$\mathbf{L} = \begin{bmatrix} e^{-x_1} L_0(x_1) & e^{-x_1} L_1(x_1) & \dots & \dots & e^{-x_1} L_{N-1}(x_1) \\ e^{-x_2} L_0(x_2) & e^{-x_2} L_1(x_2) & \dots & \dots & e^{-x_2} L_{N-1}(x_2) \\ \vdots & \vdots & \dots & \dots & \vdots \\ e^{-x_{N-1}} L_0(x_{N-1}) & e^{-x_{N-1}} L_1(x_{N-1}) & \dots & \dots & e^{-x_{N-1}} L_{N-1}(x_{N-1}) \\ e^{-x_N} L_0(x_N) & e^{-x_N} L_1(x_N) & \dots & \dots & e^{-x_N} L_{N-1}(x_N) \end{bmatrix} \quad (25)$$

Inverting this matrix (see appendix 6.1), then applying \mathbf{L}^{-1} to both sides of equation 24.

$$\sum_{k=1}^N \mathbf{L}_{nk}^{-1} R_{N-1}(x_k) = \alpha_n. \quad (26)$$

Evaluating 26 for $n = 0$, then inserting into equation 23 gives

$$\int_0^\infty W(x)g(x)dx \approx \int_0^\infty e^{-x} R_{N-1}(x)dx = \sum_{k=1}^N \mathbf{L}_{0k}^{-1} L_{2N-1}(x_k) \quad (27)$$

which, when defining the weights as $\omega_k = \mathbf{L}_{0k}^{-1}$ gives the final equation

$$\int_0^\infty W(x)g(x)dx \approx \sum_{k=1}^N \omega_k g(x_k) \quad (28)$$

and $\{x_k | k \in \{1, \dots, N\}\}$ being the zeros of the Laguerre polynomial L_N of degree N . Going back, equation 22 can now be approximated as

$$C \int_0^\infty W(r_1)R(r_1)dr_1 \approx \sum_{k=1}^N \omega_k R(r_1). \quad (29)$$

The same is done for the variable r_2 of course, and as for the other variables; each of them can be approximated by the Gauss- Legendre quadrature with a simple change of variables as showcased in 3.1.

3.2 Monte Carlo Integration

A different approach to solving integrals numerically is the use of Monte Carlo integration, where properties of probability distribution functions (PDFs) are used to approximate the solution. For any integral $\int_a^b f(x)dx$, one can find a PDF $p(x)$ that fulfills $\int_a^b p(x)dx = 1$ that is nonzero $\forall x \in [a, b]$ Then by the law of large numbers [1],

$$\int_a^b f(x)dx = \int_a^b p(x) \frac{f(x)}{p(x)} dx = E \left[\frac{f(x)}{p(x)} \right] \approx \frac{1}{N} \sum_{i=1}^N \frac{f(x_i)}{p(x_i)}$$

where N is a very large number and x_i are N random samples from the given PDF.

The variance is then given by

$$\sigma^2 = \frac{1}{N} \sum_{i=1}^N \left(\left(\frac{f(x_i)}{p(x_i)} \right) - E \left[\frac{f(x)}{p(x)} \right] \right)^2 p(x_i) = E \left[\left(\frac{f(x)}{p(x)} \right)^2 \right] - E \left[\frac{f(x)}{p(x)} \right]^2$$

It can then be shown [1] that the standard error of the mean is

$$\sigma_N \approx \frac{\sigma}{\sqrt{N}}$$

Thus, the error is a function of $\frac{1}{\sqrt{N}}$. This is not dependent on the dimensionality of the integral to be evaluated, making Monte Carlo methods very effective for

integrals in higher dimensions. For Monte Carlo integration in more than one dimension, the only thing that needs to be changed is that each variable needs its own independent PDF. For two variables x and y , for example, we have that

$$\begin{aligned}\int_a^b f(x, y) dx dy &= \int_a^b p_1(x) p_2(y) \frac{f(x, y)}{p_1(x) p_2(y)} dx dy = E \left[\frac{f(x, y)}{p_1(x) p_2(y)} \right] \\ &\approx \frac{1}{N} \sum_{i=1}^N \frac{f(x_i, y_i)}{p_1(x_i) p_2(y_i)}\end{aligned}$$

where N is a very large number and x_i, y_i are random samples from their respective PDFs.

The appropriate choice of a fitting PDF is crucial. Even though the above equations hold true for any PDF, choosing a PDF $p(x)$ that closely follows our function $f(x)$, leads to a better sampling of x_i [1] and decreases the standard deviation. Thus, the real integral is approached much faster.

In order to generate random variables x_i that have the same distribution like $p(x)$, we require that the cumulative distribution function (CDF) $P(x)$ belonging to $p(x)$ is invertible. We have then that $P^{-1}(U)$, where U is standard uniformly distributed, generates random variables x_i that have the same distribution as $p(x)$ (see Appendix 6.2).

Standard uniformly distributed pseudo- random variables can be generated with a random number generator.

3.3 Application

3.3.1 Legendre polynomials

The first approach to solving the integral is to use Legendre polynomials. As Legendre polynomials cannot be properly mapped to $(-\infty, \infty)$, it is necessary to define a threshold λ where the integrand is "sufficiently" zero. Thus, the integral is only evaluated for $(-\lambda, \lambda)$. As can be seen in Figure 1, the integrand approaches zero rather quickly, and $\lambda=2$ seems to be an appropriate choice.

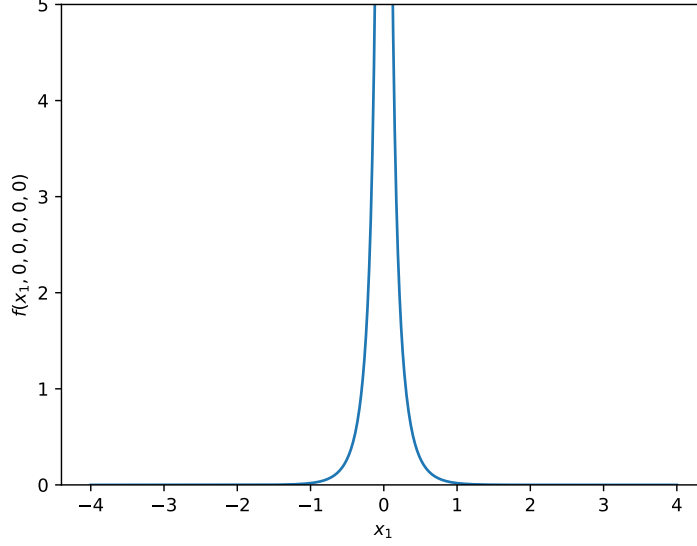


Figure 1: Plot of the integrand as a function of x_1 when $x_2 = y_1 = y_2 = z_1 = z_2 = 0$.

The integration limit is then changed to $[-2, 2]$ for all 6 integrands. It is then possible to map the Legendre functions from $[-1, 1]$ to $[-2, 2]$. Because any of the 6 variables in the integral are freely interchangeable, the approximation then reads,

$$\begin{aligned}
& \int_{-\infty}^{\infty} \int_{-\infty}^{\infty} \int_{-\infty}^{\infty} \int_{-\infty}^{\infty} \int_{-\infty}^{\infty} \int_{-\infty}^{\infty} f(x_1, x_2, y_1, y_2, z_1, z_2) dx_1 dx_2 dy_1 dy_2 dz_1 dz_2 \\
& \approx \int_{-2}^2 \int_{-2}^2 \int_{-2}^2 \int_{-2}^2 \int_{-2}^2 \int_{-2}^2 f(x_1, x_2, y_1, y_2, z_1, z_2) dx_1 dx_2 dy_1 dy_2 dz_1 dz_2 \\
& \approx \sum_{i=1}^N \sum_{j=1}^N \sum_{k=1}^N \sum_{l=1}^N \sum_{m=1}^N \sum_{n=1}^N \omega_i \omega_j \omega_k \omega_l \omega_m \omega_n f(x_i, x_j, x_k, x_l, x_m, x_n)
\end{aligned}$$

where x_i and ω_i are the weights and the mesh points from the Gauss- Legendre quadrature and f is the function to be integrated in Cartesian coordinates. This will lead to a total of N^6 function evaluations. A possible problem to face is that one will end up dividing by zero N^3 times. This problem can be faced by ignoring all function evaluations where the function's denominator is lower than a threshold, which was chosen to be 10^{-8} .

3.3.2 Laguerre and Legendre polynomials

When transferred into spherical coordinates, the integral reads

$$\int_0^\pi \int_0^\pi \int_0^{2\pi} \int_0^{2\pi} \int_0^\infty \int_0^\infty \frac{r_1^2 r_2^2 \sin(\theta_1) \sin(\theta_2) e^{-4(r_1+r_2)}}{\sqrt{r_1^2 + r_2^2 - 2r_1 r_2 \cos(\beta)}} dr_1 dr_2 d\phi_1 d\phi_2 d\theta_1 d\theta_2$$

with

$$\cos(\beta) = \cos(\theta_1)\cos(\theta_2) + \sin(\theta_1)\sin(\theta_2)\cos(\phi_1 - \phi_2)$$

This has the advantage that infinity only has to be faced twice, and Laguerre-Polynomials can be used for that. Laguerre-polynomials are defined for $[0, \infty)$ and have a weight function $W(x) = e^{-x}$. This is relevant for r_1 and r_2 , as the integration limits go from 0 to ∞ . The angles θ_1 and θ_2 lie in $[0, \pi]$, and the angles ϕ_1 and ϕ_2 lie in $[0, 2\pi]$. Here, Legendre-Polynomials can be used again. Because each of the θ , ϕ and r are interchangeable, it is necessary to create 3 types of mesh points and weights: One using the Laguerre polynomials (ω_r , x_r), one using Legendre polynomials for the angle θ (ω_θ , x_θ) and one using Legendre polynomials for the angle ϕ (ω_ϕ , x_ϕ). The function to be evaluated changes slightly due to the Laguerre-polynomials weight function, the exponent goes from -4 to -3, leading to

$$g(r_1, r_2, \theta_1, \theta_2, \phi_1, \phi_2) = \frac{r_1^2 r_2^2 \sin(\theta_1) \sin(\theta_2) e^{-3(r_1+r_2)}}{\sqrt{r_1^2 + r_2^2 - 2r_1 r_2 \cos(\beta)}}$$

$$\int_0^\pi \int_0^\pi \int_0^{2\pi} \int_0^{2\pi} \int_0^\infty \int_0^\infty g(r_1, r_2, \theta_1, \theta_2, \phi_1, \phi_2) dr_1 dr_2 d\phi_1 d\phi_2 d\theta_1 d\theta_2$$

This integral is then approximated by the following sum:

$$\approx \sum_{i=1}^N \sum_{j=1}^N \sum_{k=1}^N \sum_{l=1}^N \sum_{m=1}^N \sum_{n=1}^N \omega_{r,i} \omega_{r,j} \omega_{\theta,k} \omega_{\theta,l} \omega_{\phi,m} \omega_{\phi,n} g(x_{r,i}, x_{r,j}, x_{\theta,k}, x_{\theta,l}, x_{\phi,m}, x_{\phi,n})$$

Again, the risk of dividing by zero is averted when the denominator is lower than a threshold, which was chosen to be 10^{-8} .

3.3.3 Monte Carlo integration without importance sampling

The first approach is to use Monte Carlo with uniformly distributed values for each dimension in the range $[-\lambda, \lambda]$, as no uniform distributions for $(-\infty, \infty)$ exist. As for the Legendre polynomials, the integration limits were changed to $[-2, 2]$ for all 6 integrands. Using the PDF $p(x)=0.25$ for $x \in [-2, 2]$, otherwise zero, the integral reads

$$\int_{-2}^2 \int_{-2}^2 \int_{-2}^2 \int_{-2}^2 \int_{-2}^2 \int_{-2}^2 0.25^6 f(x_1, x_2, y_1, y_2, z_1, z_2) dx_1 dx_2 dy_1 dy_2 dz_1 dz_2$$

$$\approx 4^6 \frac{1}{N} \sum_{i=1}^N f(x_{i,1}, x_{i,2}, x_{i,3}, x_{i,4}, x_{i,5}, x_{i,6})$$

where $x_{i,1}, \dots, x_{i,6}$ are uniformly distributed in $[-2, 2]$. Again, all function evaluations where the denominator is smaller than 10^{-8} , are ignored.

3.3.4 Monte Carlo integration with importance sampling

In polar coordinates, the polar part of the function resembles the PDF $p(r_1, r_2) = 16e^{-4(r_1+r_2)}$, where $p(r_1, r_2)$ is the product of two exponential distributions with

parameter=4. Thus, it is possible to sample both r_1 and r_2 from that exponential distribution. The angles θ_1 and θ_2 can be sampled from a uniform distribution for values in $[0, \pi]$, while the angles ϕ_1 and ϕ_2 are taken from a uniform distribution for values in $[0, 2\pi]$. Doing this, the function that we want to get the expectation value from is given by

$$g(r_1, r_2, \theta_1, \theta_2, \phi_1, \phi_2) = \pi^4 \frac{2^2}{4^2} \frac{r_1^2 r_2^2 \sin(\theta_1) \sin(\theta_2)}{\sqrt{r_1^2 + r_2^2 - 2r_1 r_2 \cos(\beta)}}$$

with $\cos(\beta)$ as defined earlier. Thus, the integral is approximated by

$$\frac{1}{N} \sum_{i=1}^N g(r_{i,1}, r_{i,2}, \theta_{i,1}, \theta_{i,2}, \phi_{i,1}, \phi_{i,2})$$

where $r_{i,1}, r_{i,2}$ are exponentially distributed with a factor 4; $\theta_{i,1}, \theta_{i,2}$ are uniformly distributed in $[0, \pi]$, and $\phi_{i,1}, \phi_{i,2}$ are uniformly distributed in $[0, 2\pi]$. In order to create exponentially distributed random variables, we use that a variable x_i is exponentially distributed when

$$x_i = -\frac{1}{4} \ln(1 - u_i)$$

where u_i is standard uniformly distributed. Again, all function evaluations where the denominator is smaller than 10^{-8} , are ignored.

3.4 Computational implementation

The computational implementation of the formulas that were found was rather straightforward. For the Legendre polynomials, Numerical Recipe's *gauleg* function was used to fill to arrays of size N with the mesh points and weights, for the Laguerre polynomials, we used Numerical Recipe's *gaulag* function [4]. The 6-fold sums were then implemented as 6-fold loops.

For the Monte Carlo integration, we used the Mersenne Twister random number generator with a randomly generated seed to create standard uniformly distributed numbers and transformed them according to the earlier described process. We tested both the Laguerre polynomials, the Legendre polynomials and Monte Carlo integration on example integrals to make sure that everything works as predicted. We then used Python scripts to analyse and plot the data we have gotten.

3.4.1 Parallelization

Because each of the 4 approaches calculates terms in a sum that are independent of each other, it is easy to parallelize the code. We made a parallelized version of each of the 4 approaches as well. The code was parallelized using MPI, and a flexible function was created by us to make sure that each thread gets the same amount of workload. That function was tested a well. The 6-fold for loops used in the Gaussian quadrature were replaced by a single while-loop with multiple if/else clauses that essentially do the same.

4 Results

4.1 Legendre polynomials

The results achieved using Legendre polynomials with a cutoff $\lambda = 2$, as well as time use for both the parallelized and the non-parallelized case, and the deviation from the correct result, can be found in table 1.

Table 1: Achieved results, relative error, time-usage in seconds (averaged over 5 simulations, but for $n=55$ and $n=65$) for both the nonparallel and the parallel program (without optimization flags on 4 cores) as well as standard error for integration using Legendre polynomials.

N	Result	Relative Error	time [s] parallelized	time [s] nonparallelized
10	0.129834	0.326466	0.021025232	0.0388234
15	0.199475	0.0348043	0.1436784	0.4376558
20	0.177065	0.0814488	0.7488488	2.70073
25	0.189110	0.018967	3.107388	-
30	0.185796	0.0361583	8.855728	29.37128
40	0.18867	0.0212464	49.99648	-
45	0.190128	0.0136823	95.06266	-
55	0.190669	0.0108763	303.598	-
65	0.191035	0.00897612	823.381	-

Even though the relative error tends to get smaller for larger values of N , even with $N=65$, there is a divergence between the analytical and the numerical result. Choosing a different threshold λ might improve the result, as would larger values of N . One interesting aspect is that, for specific values of N ($N = 15$, $N = 25$), one gets more correct results than for larger values of n . This is presumably caused by us ending up getting "lucky" mesh points and weights. However, none of the results give close results, and the error is in the third decimal.

4.2 Laguerre and Legendre polynomials

The results achieved using Laguerre Polynomials for the radial parts and Legendre polynomials for the angle parts of the spherical integral as well as time use for both the parallelized and the nonparallelized case, and the deviation from the correct result, can be found in table 2.

Table 2: Achieved results, relative error, time-usage in seconds (averaged over 5 simulations, but for $n=55$ and $n=65$) for both the nonparallel and the parallel program (without optimization flags on 4 cores) as well as standard error for integration using Laguerre polynomials (for the radial parts).

N	Result	Relative Error	time [s] parallelized	time [s] nonparallelized
10	0.177081	0.0813679	0.05331922	0.1115982
15	0.193285	0.00269565	0.3914072	1.200048
20	0.194786	0.0104784	2.044996	7.023426
25	0.194804	0.0105751	8.18345	-
30	0.194779	0.010443	25.8677	81.0227
40	0.194669	0.009873	142.9906	-
45	0.194594	0.00948246	269.7448	-
55	0.194439	0.00868232	884.532	-
65	0.194298	0.00794811	2429.59	-

Compared to the Cartesian Legendre polynomials case, even quite small values of N give good estimates for the total result. However, for larger values of N , we did not achieve much better results than with using Legendre polynomials, which is surprising, given that the correct integration limits are taken into account. It is also quite interesting to see that evaluating the Laguerre polynomials takes roughly 3 times as much time as the Legendre polynomials. This might be caused by the computer system having to look up in different arrays, or by the more complex function that is evaluated. Again, for $N = 15$, one gets a surprisingly correct result, which is presumably caused by lucky mesh points.

4.3 Cartesian Monte Carlo without importance sampling

The results achieved using Monte Carlo simulation and uniform distributions for Cartesian coordinates as well as time use for both the parallelized and the nonparallelized case, and the deviation from the correct result and the standard error σ^2/\sqrt{N} , can be found in table 3.

Table 3: Achieved results, relative error, time-usage in seconds (averaged over the 5 parallel simulations) for both the nonparallel and the parallel program (without optimization flags on 4 cores) as well as standard error for different values of N for Cartesian Monte Carlo without importance sampling. The result with the median relative error is presented, the standard error is calculated from the averaged variance over the 5 parallel runs.

N	Result	Relative Error	time [s] parallelized	time [s] nonparallelized	Standard Error
10^3	0.122134	0.366414	0.0003482432	0.0003056	0.1344
10^4	0.140808	0.269539	0.002769808	0.0034032	0.2318
10^5	0.20568	0.066995	0.02500496	0.0328912	0.02865
10^6	0.183756	0.046738	0.10475636	0.3262482	0.008598
10^7	0.191025	0.00902881	0.8515582	3.090702	0.006693
10^8	0.192471	0.00152991	8.520786	29.38188	0.0009739
10^9	0.192261	0.00261722	91.32978	-	0.0003159

As expected, larger values of N lead to more correct results, and the standard error goes down (but for $N = 10^4$, where the result is completely off. However, this only happened for one of the 5 simulations). Compared to the Legendre polynomials, that solve exactly the same integral, the results are closer to the real result. However, the result for $N = 10^9$, which is 0.192261, is more than one standard error smaller than the analytical solution, which can give the wrong impression that this wrong result indeed is correct. This is due to the fact that parts of the integral are omitted. Choosing a larger threshold value λ would likely lead to a more correct result, but we did not test this further.

4.4 Spherical Monte Carlo with importance sampling

The results achieved using Monte Carlo simulation with importance sampling as described earlier in spherical coordinates as well as time use for both the parallelized and the nonparallelized case, and the deviation from the correct result and the standard error σ^2/\sqrt{N} , can be found in table 4.

Table 4: Achieved results, relative error, time-usage in seconds (averaged over the 5 parallel simulations) for both the nonparallel and the parallel program (without optimization flags on 4 cores) as well as standard error for Cartesian Monte Carlo with importance sampling. The result with the median relative error is presented, the standard error is calculated from the averaged variance over the 5 parallel runs.

N	Result	Relative Error	time [s] parallelized	time [s] nonparallelized	Standard Error
10^3	0.220074	0.141665	0.0005288586	0.0004486	0.05248
10^4	0.197875	0.0265038	0.00493595	0.0048254	0.009458
10^5	0.195131	0.0122716	0.03278686	0.0480236	0.003511
10^6	0.192313	0.00234779	0.158712	0.4711302	0.001036
10^7	0.193096	0.00171425	1.236776	4.575088	0.0003362
10^8	0.192688	0.000403855	13.06474	42.41482	0.0001037
10^9	0.192784	9.70237E-05	141.535	-	$3.287 \cdot 10^{-5}$

As expected, increasing N leads to more correct results. Compared to the other methods, this method leads to the most correct result, and we ended up having $0.192784 \pm 3.287 \cdot 10^{-5}$ as our final result. Even for comparatively small values of N , such as $N = 10^7$, the achieved result is closer to the analytical solution, and for $N = 10^9$, the standard error is in the magnitude of $N = 10^{-5}$, with a result that is close enough to the analytical solution to be used further.

4.5 Time usage and parallelization

Figure 2 plots the relative error (in log-scale) of the different algorithms against the time use (in log-scale) for the parallelized algorithms.

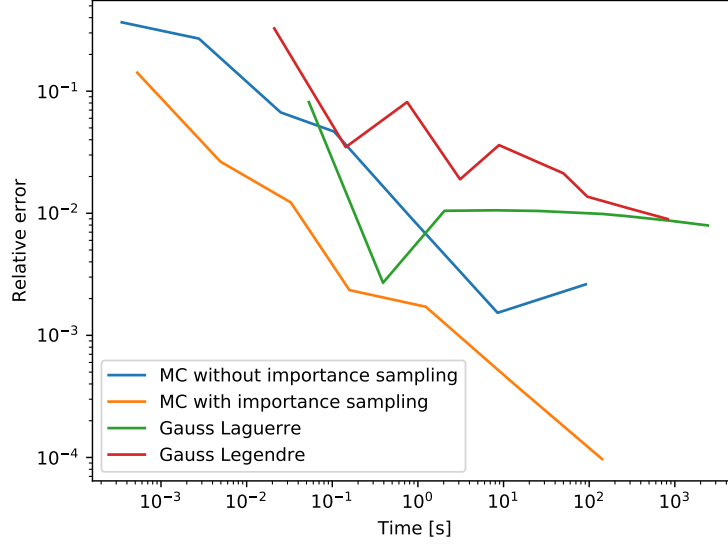


Figure 2: Time usage [s] of parallelized algorithms plotted against the methods' relative error. Logarithmic scales for both axes were used. The data from the tables 1-4 was used.

This graph clearly shows that both Monte Carlo approaches lead to better results than the Gaussian quadrature methods, but for the "lucky" result in the Laguerre results. It also shows that clever importance sampling can further decrease the relative error in a magnitude of almost 10^{-2} , compared to the other Monte Carlo approach. It also gives the impression that neither of the quadrature approaches would lead to much better results, even upon increasing N , while the Monte Carlo methods, especially the one with importance sampling, could decrease the error even further. It should be mentioned that a possible reason why the Monte Carlo approach without importance sampling gives a worse result for its most time consuming calculation (with $N = 10^9$), might be due to the way the represented value was chosen - the median value.

Figure 3 plots the value N against the relative difference in time use when the nonparallelized algorithm is compared to the parallelized algorithm for the Monte Carlo case with importance sampling.

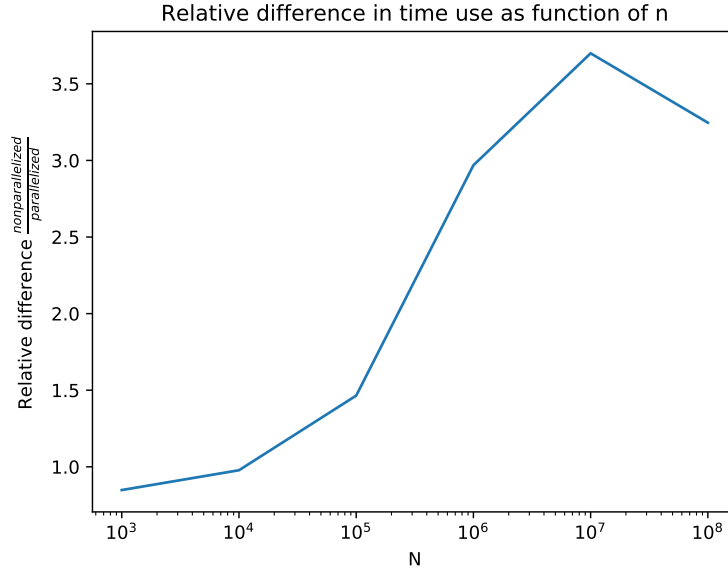


Figure 3: N (logarithmic scale) plotted against the relative difference in time use between the nonparallelized and the parallelized algorithm. Data from table 4 was used.

One can clearly see how parallelization, or at least the way we implemented it, does not give faster results for small values of N . To the contrary, for N up to 10^4 , parallelization increases the average run time. However, for larger values of N , such as 10^8 , parallelization makes the program run 3 to 3.5 times faster. This is less than theoretically possible (one could get a boost of up to 4 on 4 identical CPU cores), but still clearly justifies the process of parallelizing a program, especially when the run times are large. The other 3 approaches gave similar results, as can be seen in tables 1-3. The reason why no perfect time enhancement was achieved probably lies in an imperfect implementation, as each process has to run some functions, that in theory do not need to be re-run several times, and in that only the time-sensitive parts are parallelized.

We also tested the impact of the "-O3" parallelization flag on the run time. The results can be seen in figure 4:

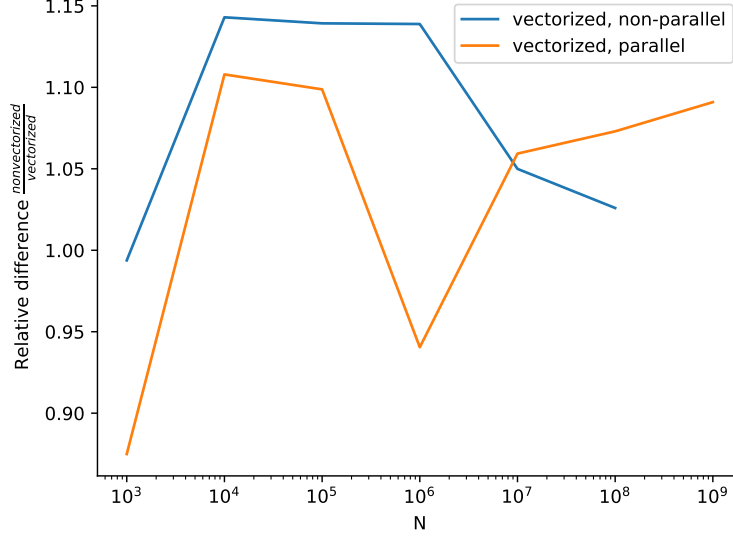


Figure 4: N (logarithmic scale) plotted against the relative difference in time use between the non-vectorized and the vectorized program.

The "-O3"-flag seems to have a small, but not negligible impact on the run time of both the parallelized and the non-parallelized code, and for large N , the compiler flag seems to give an additional speed boost. However, that behaviour is quite erratic, and the time improvement is very small, making this data not completely reliable. It is possible that careful coding of loops could improve these results.

5 Conclusion

The application of Gauss- Legendre quadrature was for this particular integral, a poor choice. In this instance, errors were introduced at several points. When approximating the function value of the integrand to be zero at inputs greater than 2, and when approximating the function by a polynomial of degree $2N - 1$. Instead, by using the more appropriate choice of the Gauss- Laguerre quadrature, for the two radial variables; those ranging from zero to infinity and Gauss- Legendre for the remaining variables through a change of variables. Errors are only introduced in approximating the function values with that of polynomials of degree $2N - 1$. However Gauss- Laguerre quadrature proved no better than Gauss- Legendre quadrature for large numbers of mesh points. This is surprising as in theory, we expected Gauss- Laguerre to produce clearly better results than Gauss- Legendre. This might be a sign of faulty implementation or simply due to the integrand 18 being less well approximated by a polynomial.

Monte Carlo integration is an excellent choice for six- dimensional integrals and higher, as the error scales with $\frac{1}{\sqrt{N}}$ for a number of mesh points N regard-

less of the dimensionality of the integral. The choice of whether or not to tailor the PDF to suit the integrand, proved to have a tremendous effect on the time expenditure and accuracy of the program, with importance sampling accounting for an approximately 97% decrease in relative error, measured at $N = 10^9$ mesh points. See appendix(6.3), but also an approximately 55% increase in time expenditure (measured for the parallelized programs at $N = 10^9$. See appendix (6.4).

The implementation of parallelization proved to be especially worth while for $N > 10^5$ as is seen in figure 3. The speed up should on the surface be 4 times greater on computers with quad- core computer chips, however factors such as writing and fetching to and from memory impacts this effect negatively, especially when moving from fast to slow memory. The effect could still be primarily because of a potentially suboptimal implementation of parallelization.

6 Appendix

6.1 Proof that \mathbf{L} is invertible

For the matrix \mathbf{L} in equation 25; each column is constructed of constants multiplied with the Laguerre polynomial L_n for each row in column n . With the Laguerre polynomials being orthogonal with respect to the inner product

$$\langle L_n | L_m \rangle = \int_0^\infty e^{-x} L_n(x) L_m(x) dx = C_{mn} \delta_{mn} \quad (30)$$

where $\langle L_n | L_m \rangle$ is the inner product of two Laguerre polynomials, δ_{mn} is the Kronecker- delta and C_{mn} is a normalization constant. no column can be expressed as a linear combination of any of the others (at least not for $x \in [0, \infty]$), so \mathbf{L} is an $N \times N$ matrix with N linearly independent columns. As such it is necessarily non-singular and therefore, must be invertible. This proof would also apply to the Legendre polynomials under a different inner product.

6.2 Proof that $F^{-1}(U)$ has cumulative function $\mathbf{F(x)}$

Let $F(X)$ be a cumulative distribution function (CDF).

Let U be standard uniformly distributed and let G be it's CDF, that is, $G(u) = u$ for $0 \leq u \leq 1$, otherwise 0.

Assume that $X = F^{-1}(U)$. Then

$$F(x) = P(X \leq x) = P(F^{-1}(U) \leq x) = P(U \leq F(x)) = G(F(x)) = F(x)$$

6.3 Monte Carlo relative error improvement with importance sampling

Relative error in the Monte Carlo method with and without importance sampling at $N = 10^9$

$$\frac{0.00261722 - 0.0000970237}{0.00261722} \cdot 100 \approx 96.3\%.$$

The absolute error decreased by approximately 96.3% when implementing importance sampling at $N = 10^9$.

6.4 Monte Carlo time expenditure increase with importance sampling

The increased time expenditure for Monte Carlo with importance sampling at $N = 10^9$

$$\frac{141.535 - 91.330}{91.330} \cdot 100 \approx 55\%.$$

The time expenditure increased by approximately 55% when implementing importance sampling at $N = 10^9$.

6.5 List of programs

All programs can be found on https://github.com/adrian2208/FYS3150_collab in the folder "project 3".

1. a.cpp - Legendre approach to solve the integral
2. b.cpp - Legendre and Laguerre approach to solve the integral
3. c.cpp - Monte Carlo approach (no importance sampling) to solve the integral
4. d.cpp - Monte Carlo approach (with importance sampling) approach to solve the integral
5. a_parallel.cpp - Parallelized version of a.cpp
6. b_parallel.cpp - Parallelized version of b.cpp
7. c_parallel.cpp - Parallelized version of c.cpp
8. d_parallel.cpp - Parallelized version of d.cpp
9. testings.cpp - Unit testing.
10. tests_main.cpp - Unit testing.
11. functions.hpp & functions.cpp - Contains functions for parallelization, and all the integrands, and some more.
12. compile_and_run.py - Compiles and runs (for many values of n , 5 times with and 5 times without vectorization flags) all files. Also runs testings once.
13. create_final_lists.py - Creates data that was used for tables 1-4 from the raw data. Should be run after compile_and_run.py.
14. databehandling.py - Creates plots from data created by create_final_lists.py.
15. plot_function.py - Plots the function.

7 References

- [1] Jay L Devore and Kenneth N Berk. *Modern mathematical statistics with applications*. Springer, 2012.
- [2] Morten Hjort-Jensen. Computational physics: Lecture notes fall 2015.
- [3] Morten Hjort-Jensen. Problem set 3 fall 2015.
- [4] William H Press, Saul A Teukolsky, William T Vetterling, and Brian P Flannery. Numerical recipes in c++. *The art of scientific computing*, 2:1002, 1992.